Defect Enhanced Carbon Monoxide Oxidation at Elevated Oxygen Pressures on a Pt/Al_2O_3 Thin Film

Daniel J. Burnett,[†] Aaron M. Gabelnick,[‡] Anderson L. Marsh,[‡] Henry D. Lewis,[†] Steven M. Yalisove,[§] Daniel A. Fischer,[||] and John L. Gland*[,†,‡]

Departments of Chemical Engineering, Chemistry, and Materials Science and Engineering, University of Michigan, Ann Arbor, Michigan 48109, and Materials Science and Engineering Laboratory, National Institute of Standards and Technology, Gaithersburg, Maryland 20899

Received: July 12, 2003; In Final Form: February 12, 2004

Carbon monoxide oxidation has been studied, using in situ soft X-ray techniques and ultrahigh vacuum (UHV) temperature-programmed reaction spectroscopy (TPRS), on a well-characterized supported platinum thin film over the 100−1000 K temperature range and in pressures ranging from UHV to 0.01 Torr. In high oxygen pressures the reaction is enhanced by oxidation at defect sites. Temperature-programmed fluorescence yield near-edge spectroscopy (TP-FYNES) studies of preadsorbed CO coverages heated in pressures of flowing oxygen, ranging from 1×10^{-5} to 1×10^{-2} Torr, have been performed. Unlike with the Pt(111) surface, the onset temperature for oxidation of a saturated coverage of CO on the platinum thin film decreases dramatically with increasing oxygen pressure. The CO oxidation onset temperature decreased from 340 K in 1×10^{-5} Torr of flowing oxygen to 230 K in 1×10^{-2} Torr of flowing oxygen. Therefore, oxidation is not limited by CO desorption for high CO coverages, and reactions at defect sites control the rate of CO oxidation at high oxygen pressures. Isothermal oxidation experiments in 0.002 Torr of flowing oxygen have yielded an activation energy of 8.5 kcal/mol. TPRS of coadsorbed carbon monoxide and oxygen has indicated a primary oxidation channel at 350 K corresponding to the oxidation of CO on Pt(111) terrace sites and minor oxidation channels above 400 K. The thin Pt/Al_2O_3 film has been characterized using both chemical and structural methods. CO and O_2 temperature-programmed desorption (TPD) experiments indicate the Pt film surface is similar to Pt(111), but with a higher defect site concentration. Plane-view and cross-section transmission electron microscopy (TEM) experiments have confirmed a 100 Å Pt film consisting of ∼450 Å, well-ordered grains, as indicated by local area electron diffraction patterns, with the (111) orientation parallel to the substrate.

Introduction

Molecular-level understanding of reaction mechanisms on solid surfaces remains an exciting challenge. From the time of Langmuir, the oxidation of carbon monoxide has been widely used as a model for bimolecular surface reactions.[1−5] Studies of this reaction are based on a desire to characterize fundamental surface reactions at a molecular level. CO oxidation has been investigated extensively on platinum single crystals;[1−9] yet, most real world applications of catalyzed CO oxidation occur on platinum catalysts composed of small metal particles on high surface area supports. To help bridge this "materials gap," recent CO oxidation experiments on more realistic platinum surfaces are beginning to emerge,[10−21] and of particular interest are those studies involving platinum on alumina supports.

The $CO + O_2$ oxidation reaction occurs via a bimolecular surface mechanism on alumina-supported platinum,[15,20] as well as on single crystals.[5] Below a certain temperature (dependent on reactant partial pressures), high CO coverages significantly reduce the sticking probability for oxygen.[5] Once CO desorbs from the surface, creating vacant adsorption sites, oxygen adsorbs more rapidly, dissociates, and reacts with the remaining CO to form CO_2. This inhibition of O_2 adsorption for high CO coverages results in CO desorption being the rate-limiting step at high CO coverages. On the surface of supported metallic Pt particles, CO oxidation occurs through a reaction between coadsorbed CO and atomic oxygen.[21] Similar mechanistic conclusions have been made for CO oxidation over a polycrystalline platinum foil[13] and for a $Pt/\alpha\text{-}Al_2O_3(0001)$ sample.[11] On a 2% Pt/Al_2O_3 catalyst, CO_2 formation began around 423 K with a maximum conversion temperature at 476 K.[15] Activation energies for this reaction were 22.5 and 14.0 kcal/mol under lean and rich conditions, respectively. On a Pt/Al_2O_3 monolith sample with preadsorbed CO, carbon dioxide production occurred at 310 K in pressures of oxygen.[12] When oxygen was preadsorbed and the monolith sample was heated in pressures of CO, there was a small low-temperature CO_2 peak at 250 K with a large broad peak beginning at 540 K.[12] In other experiments on a wide variety of Pt/Al_2O_3 surfaces, experimental activation energies obtained have ranged from 7.2 to 29.0 kcal/mol.[16] Below 500 K, experimental activation energies obtained have ranged from 7.2 to 15.0 kcal/mol.[16]

To understand high-pressure catalytic processes, species present on the surface under reactive atmospheres must be characterized. This "pressure gap" is bridged through direct, molecular-level characterizations, and in recent years in situ

* Corresponding author. Address: 930 N. University Ave., Ann Arbor, MI 48109. Phone: 734-764-7354. Fax: 734-647-4865. E-mail: gland@umich.edu.

[†] Department of Chemical Engineering, University of Michigan.

[‡] Department of Chemistry, University of Michigan.

[§] Department of Materials Science and Engineering, University of Michigan.

[||] National Institute of Standards and Technology.

10.1021/jp036012z CCC: $27.50 © 2004 American Chemical Society
Published on Web 04/03/2004

studies have become increasingly feasible.[22,23] Several groups have extrapolated low-pressure CO oxidation data to higher pressures.[7,24,25] However, there is experimental evidence that the extrapolation of kinetic data from model low-pressure experiments to high-pressure conditions results in incomplete models that do not include the effects of weakly adsorbed species.[26] In addition to these studies, other groups have reported experimental reaction data over a broader range of pressures.[27,28]

This work reports results for CO oxidation on a Pt/Al_2O_3 thin film as part of our program to characterize catalytic mechanisms of light hydrocarbon oxidation on platinum surfaces in pressures of flowing oxygen.[29−33] Thin films are interesting models for small particles and support effects present on supported platinum catalysts.[34] Thin Pt films are also valuable as sensing films for chemical sensors for fuels in air.[35] For example, Pt/Al_2O_3 and Pt/TiO_{2-x} thin films have been used to detect propylene and benzene in air.[36] The film used in this work has been characterized both chemically and structurally. The reaction between CO and oxygen has been explored using classical low-pressure surface science experiments combined with in situ soft X-ray studies capable of characterizing reactions under reactive atmospheres. This combination of techniques has provided detailed information on the role of defects during CO oxidation on platinum catalyst surfaces.

Experimental Section

The 100 Å Pt/350 Å Al_2O_3 thin film was grown on a 4 in. Si wafer covered with a thick (∼10 μm) layer of thermally grown SiO_2. The 100 Å Pt film was evaporated onto a 350 Å Al_2O_3 layer sputter-deposited onto the SiO_2/Si wafer. After deposition of the thin film layers, the sample was treated with a rapid thermal anneal to 873 K in Ar. A 1 cm^2 section of the thin film sample was used in these experiments.

Experiments conducted on the U7A beamline at the National Synchrotron Light Source (NSLS) at Brookhaven National Laboratory used a detector optimized for fluorescence at the C K-edge.[37] The U7A beamline is described in detail elsewhere.[29] The Pt/Al_2O_3 film was clamped to a Ta foil backing mounted on Ta wire supports attached to the end of a 1.8-m liquid nitrogen cooled re-entrant manipulator. Temperature was measured with a type K thermocouple spot welded to the Ta foil and was controlled using a RHK temperature controller. The thin film was initially cleaned by heating to 600 K in 0.002 Torr of O_2 for 60 s, followed by a 20 s anneal at 1000 K. Gases were dosed into the background using leak valves, and flow was maintained throughout reactivity experiments using a throttled turbo pump. Fluorescence yield spectra were recorded with 150 μm/150 μm slits, yielding an overall energy resolution of 0.4 eV. Kinetic, or transient, experiments were performed with 450 μm/450 μm slits, yielding a 1.2 eV energy resolution, to improve time resolution and signal-to-noise. All temperature-programmed soft X-ray fluorescence experiments used a heating rate of 0.5 K/s, which allows for 2−3 K resolution during the experiments. Repeated experiments indicate that thermal transitions are reproducible to 2 K. Fluorescence yields at the carbon continuum (330 eV) from saturated CO coverages were monitored daily to guarantee reproducibility of intensities. All transient experiments were performed at 287.8 eV (CO π^* resonance) and at normal incidence of the electric field vector with respect to the surface normal.

Temperature-programmed fluorescence yield near-edge spectroscopy (TP-FYNES) experiments were conducted in the following manner. First, the film was cleaned by heating to 600 K in oxygen. Then the film was flashed to 1000 K in vacuum. To obtain a saturated coverage of CO, the film was ballistically cooled in a background pressure of carbon monoxide (2×10^{-7} Torr). The uptake of CO was measured during cooling by monitoring the fluorescence yield. When the surface concentration reached the desired level, the exposure was terminated. Oxygen was introduced, the ion gauge was turned off, and the oxygen pressure was monitored with a 1 Torr capacitance manometer. Reaction pressures were achieved using a combination of turbo pump throttling and leak valve control. Once the desired oxygen pressure was reached and stabilized, the film was resistively heated from 100 to 600 K while the fluorescence intensity was monitored at 287.8 eV. Absolute carbon coverage was determined by comparing fluorescence yields of CO on the Pt/Al_2O_3 film with fluorescence yields of CO on Pt(111) at the same resonance. Because the absolute carbon coverage for a saturated CO coverage on Pt(111) is known (9.6×10^{14} CO molecules/cm^2),[38] absolute surface carbon coverages have been obtained for CO on the Pt thin film.

Kinetic parameters were obtained through a series of isothermal oxidation experiments. The film was cleaned, cooled, and dosed with a saturated coverage of CO as in the TP-FYNES experiments described above. The film was then rapidly heated in 0.002 Torr of flowing oxygen to the desired reaction temperature and stabilized (±0.5 K). The CO concentration was monitored as a function of time using the fluorescence intensity at 287.8 eV. To obtain kinetic parameters, the concentration versus time data was fit to an appropriate decay curve. By performing a series of kinetic experiments at selected oxygen pressures and reaction temperatures, the activation energies and prefactors were determined.

Temperature-programmed reaction spectroscopy (TPRS) and desorption (TPD) experiments were performed at the University of Michigan in an ultrahigh vacuum chamber equipped with rough, ion, turbomolecular, and titanium sublimation pumps to achieve a base pressure of 1×10^{-10} Torr. The chamber is outfitted with a quadrapole mass spectrometer (QMS) and Auger electron spectrometer (AES). AES was used to verify the cleanliness of the thin film. Details of this experimental system and the TPRS/TPD experiments are available in the literature.[39] All TPRS and TPD experiments were performed using a 5.0 K/s heating rate. Gas exposures are reported in langmuirs (L) and are uncorrected for the ionization gauge sensitivity.

Structural characterization of the Pt film by transmission electron microscopy (TEM) was carried out using a JEOL 4000 EX transmission electron microscope operating at 400 kV. Cross-section TEM samples were prepared by substrate cleavage, mechanical thinning to ∼50 μm, polishing, and ion milling (3 kV Ar^+) to perforation. Plane-view TEM samples were prepared by ultrasonic cutting, mechanical thinning to ∼125 μm, and chemical etching from the backside to perforation.

Results

Characterization Using CO and O_2 Chemisorption. CO and O_2 TPD experiments have been completed to chemically characterize the Pt thin film surface. A series of CO TPD experiments for selected CO exposures is shown in Figure 1. For all coverages, CO desorbs from the Pt/Al_2O_3 surface with a main peak between 400 and 600 K. For the saturated CO coverage (2.0 L exposure), the main desorption peak begins around 350 K, peaks at 432 K, and is complete by 625 K. As the coverage decreases, the peak maximum increases in temperature to 547 K for the lowest CO coverage (0.05 L exposure). As seen in Figure 1, the main desorption peak is followed by a high-temperature shoulder, which remains around 575 K even for the lowest coverage studied. This peak is associated with

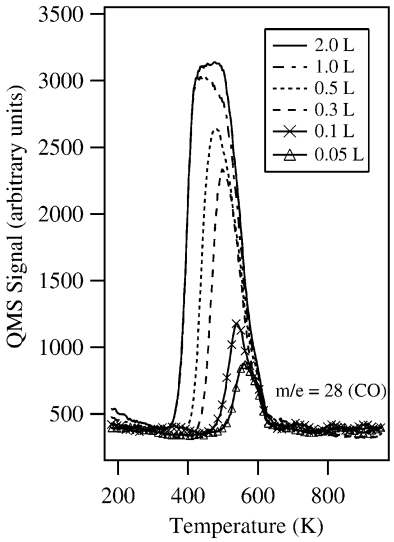

Figure 1. TPD spectra of selected CO coverages from a 100 Å Pt/350 Å Al_2O_3 thin film.

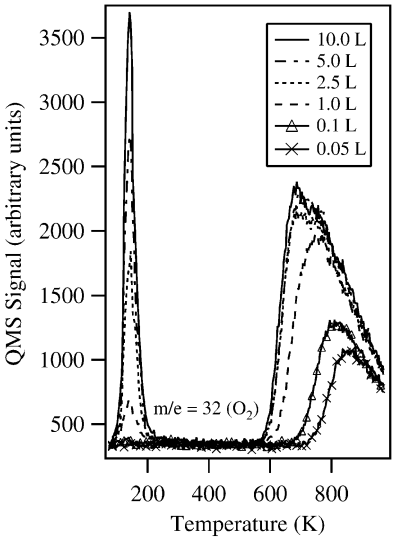

Figure 2. TPD spectra of selected O_2 coverages from a 100 Å Pt/350 Å Al_2O_3 thin film. Molecular oxygen desorbs in a sharp peak below 230 K, whereas atomic oxygen recombines and desorbs in a broad peak above 600 K.

the desorption of tightly bound CO, where CO adsorbs on low-coordination platinum sites (i.e., steps, kinks, and other defect sites). With the Redhead method,[40] the CO desorption energy ranges from 32.6 kcal/mol for a saturated coverage to 42.4 kcal/mol for low coverages.

Figure 2 shows a series of molecular oxygen TPD experiments performed over a wide range of oxygen coverages (0.05−10 L exposures). As observed in Figure 2, there are two oxygen desorption peaks present. The sharp, low-temperature (140 K) desorption peak results from molecular oxygen desorption. In this same temperature range, molecular oxygen dissociates on platinum and the remaining atomic oxygen becomes accommodated on the surface.[41] The broad, high-temperature (above 550 K) desorption peak corresponds to desorption of recombining atomic oxygen. For low oxygen coverages, all of the oxygen dissociates at low temperature and then recombines and desorbs above 550 K. With increasing oxygen coverage, a larger fraction of the molecular oxygen desorbs at 140 K, whereas the remaining oxygen dissociates, then recombines and desorbs above 550 K.

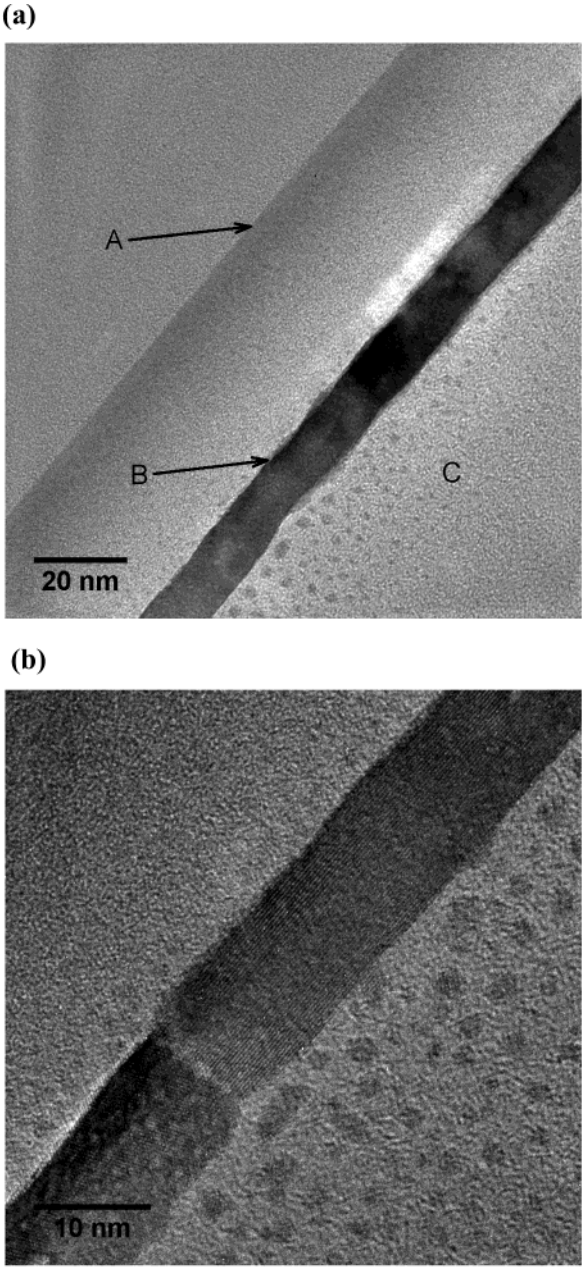

Figure 3. (a) Cross-section TEM micrograph for the Pt/Al_2O_3 film showing a 100 Å thick Pt continuous film on 350 Å alumina. (A) denotes the SiO_2/Al_2O_3 interface, (B) indicates the Al_2O_3/Pt interface, and (C) designates the glue used to bind two cleaved sections of film together. (b) Cross-section TEM micrograph of the Pt film showing flat, parallel crystalline grains.

Together, these CO and O_2 TPD results produce a clear picture of the chemistry of the Pt thin film surface. Comparisons to CO and O_2 desorption studies on single crystals indicate that the Pt thin film is similar to the Pt(111) surface with an approximate 5% defect site concentration. In addition to the chemical characterization techniques presented above, the Pt film has been structurally characterized using TEM. As indicated in the following paragraphs, these direct physical methods show that exposed (111) surfaces are predominant.

Characterization Using Transmission Electron Microscopy. A cross-section bright-field TEM micrograph of the Pt/Al_2O_3 film (Figure 3a) reveals the actual thickness of the platinum and alumina layers on the thick SiO_2 layer (∼10 μm). In Figure 3a, (A) points to the SiO_2/Al_2O_3 interface, (B) indicates the Al_2O_3/Pt interface, and (C) is the glue used to hold the two

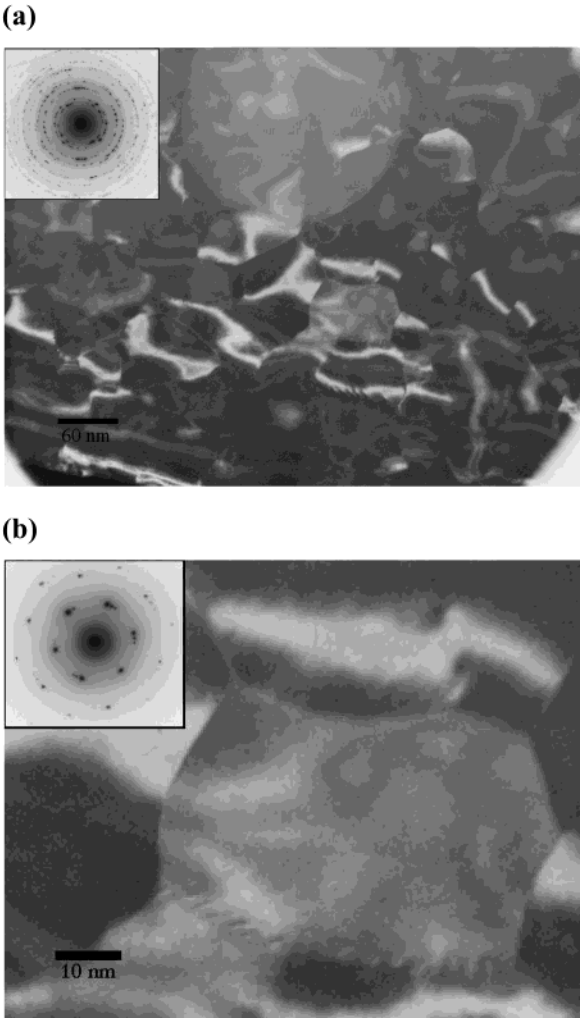

Figure 4. (a) Bright-field, plane-view image of the Pt/Al_2O_3 film. The average Pt grain size is ~450 Å. Inset depicts plane-view SAD pattern of same area of film. (b) Bright-field, plane-view micrograph and SAD pattern (inset) from a large Pt grain with a small contribution from neighboring grains. Ring/spot indexing suggests a (111) textured Pt film.

sections of film together. The average thickness of the continuous Pt layer is 100 Å, whereas the Al_2O_3 thickness is roughly 350 Å. A more detailed TEM micrograph of the Pt layer is shown in Figure 3b. The surface of the Pt film is relatively flat and parallel to the Al_2O_3 substrate. Grain boundaries and lattice fringes indicate the Pt film is crystalline in nature. Close inspection of the Pt grains reveals an average grain size greater than 400 Å.

A plane-view TEM micrograph (Figure 4a) shows a bright-field image of the Pt film, indicating a continuous array of Pt grains with an average grain size of ~450 Å. A plane-view selected area diffraction (SAD) pattern (inset in Figure 4a) reveals several distinct diffraction rings. These rings have been indexed using SAD patterns and literature *d* spacings from Si(100) as a reference standard.[42] The calculated *d* spacings from the diffraction rings, along with possible correlations to literature *d* spacings of Pt,[43] Al_2O_3,[44] and Si are shown in Table 1. The only possible platinum planes detected are Pt(311), Pt(420), Pt(220), and Pt(422). However, all of these rings closely matched *d* spacings from alumina planes.

To remove the alumina signal from the SAD pattern, a SAD pattern has been taken from a large Pt grain (Figure 4b) using a small selected area aperture. (There was a small contribution from neighboring grains because the smallest aperture available was slightly larger than the grain.) This analysis has been performed on several Pt grains, all of which produced the same SAD pattern seen in the inset of Figure 4b. The SAD pattern clearly indicates the Pt grains have 6-fold symmetry. The calculated *d* spacings from the first two diffraction spots in Figure 4b (inset) are 1.39 and 0.800 Å. These calculated *d* spacings are also found in Table 1 and correspond closely with literature values for the Pt(220) and Pt(422) planes, respectively. The Pt(311) and Pt(420) planes are not present in any of the SAD patterns from single Pt grains, suggesting that the rings at 1.18 and 0.880 Å in Figure 4b most likely result from alumina, not platinum.

TABLE 1: Calculated and Literature *d* Spacings

d (Å) measured	*d* (Å) literature	material (plane)
2.37	2.38	alumina (110)
	2.26	**Pt(111)**
1.97	1.92	Si(220)
1.39	1.39	Pt(220)
	1.37	alumina (125)
	1.35	SI(400)
1.18	1.19	alumina (220)
	1.18	Pt(311)
	1.13	**Pt(220)**
0.962	0.960	Si(440)
0.880	0.880	alumina (413)
	0.880	Pt(420)
0.800	0.801	Pt(422)
	0.799	alumina (054)

There are several Pt rings/spots missing from the SAD patterns shown in Figure 4a,b. In particular, there are no spots/rings corresponding to the Pt(111) or Pt(222) planes at the literature *d* spacings of 2.26 and 1.13 Å, respectively. The absence of these planes suggests that the wide area SAD pattern is only sampling grains that are aligned with the (111) zone axis. Hence, the film is highly textured out of the plane of the film. The fact that the individual grains exhibit a random in-plane orientation suggests a random in-plane texture. This structure is also evident in the bright-field plane-view sample in Figure 4a, where diffraction contrast varies from grain to grain.

Temperature-Programmed Reaction Spectroscopy. TPRS experiments of coadsorbed CO and O_2 have been performed for a wide range of initial carbon monoxide and oxygen coverages. Figure 5 displays a typical TPRS experiment where a partial coverage of CO is preadsorbed on the surface, followed by a saturation dose of molecular oxygen. As seen in the CO_2 ($m/e = 44$) trace, the main oxidation channel begins at 230 K, peaks at 315 K, and is complete by 380 K. Two minor carbon dioxide peaks appear at 430 and 545 K. The oxygen trace shows two desorption peaks: a molecular oxygen desorption peak centered at 141 K and a broad recombinative atomic oxygen desorption peak centered at 870 K. The presence of this recombinative atomic oxygen desorption peak after the CO_2 desorption peaks indicates that oxygen was in excess on the surface for this experiment. The small CO desorption peak at 315 K is a fragment of the 315 K CO_2 desorption peak, as the CO and CO_2 desorption peak temperatures match exactly.

Figure 6 displays a series of TPRS experiments where selected amounts of CO were preadsorbed onto the platinum surface followed by a saturation postexposure of molecular oxygen. As observed in Figure 6, the amount of oxygen adsorbed increases with decreasing CO preexposure. With a saturation preexposure of CO (trace a) oxygen adsorption is inhibited. However, as indicated by the small CO_2 signal

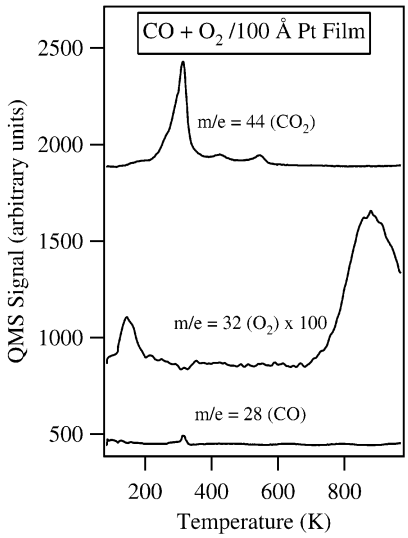

Figure 5. TPRS of coadsorbed CO and O_2. The sample was predosed with CO followed by a postexposure of oxygen. The main oxidation peak occurs at 315 K with minor oxidation peaks around 445 and 530 K.

observed above 400 K, a small amount of oxygen does adsorb and react with preadsorbed CO. When partial coverages of CO are preadsorbed, much larger concentrations of oxygen adsorb onto the surface. For traces a−c, CO is in excess, whereas for traces d and e, oxygen is in excess, as indicated by the recombinative atomic oxygen desorption peaks above 600 K. Oxygen desorption is similar to that from the clean Pt film, as shown in Figure 2.

The carbon dioxide traces shown in Figure 6 display several oxidation peaks over the 260−550 K temperature range. The main CO_2 peak begins by 260 K, peaks near 315 K, and is complete by 390 K. Peak temperatures vary slightly depending on surface concentrations of the two reactants. CO is in excess for traces a and b, as indicated by the CO desorption peaks above 400 K, and oxygen is in excess for traces d and e, as illustrated by the recombinative atomic oxygen desorption peaks above 650 K. In trace c, the CO and oxygen surface concentrations are near stoichiometric levels (slight excess of CO). Again, there are minor oxidation peaks around 430 and 545 K, which may occur from oxidizing the more tightly bound CO, which desorbs around 575 K (see Figure 1). Unreacted CO desorbs between 350 and 650 K (traces a and b), indicating CO is in excess. There is a high-temperature shoulder around 575 K, suggesting that tightly bound CO is present. As in seen Figure 5 and mentioned previously, the small CO desorption peaks at 310 K are fragment peaks from the large CO_2 signal at this temperature.

Fluorescence Yield Near-Edge Spectroscopy. The fluorescence yield near-edge spectroscopy (FYNES) data for a saturated coverage of CO adsorbed on the Pt film surface is shown in Figure 7. The upper trace shows the FY spectrum recorded at glancing incidence (30°), and the lower trace displays the FY spectrum collected at normal incidence (90°). As observed in the normal incidence spectrum, there is a large π^* peak at 287.8 eV, and no σ^* peak appears near 303.0 eV. In contrast, the glancing spectrum has a large σ^* peak at 303.0 eV, and the π^* peak at 287.8 eV has decreased in intensity relative to the step edge. Together, these results indicate that CO is adsorbed perpendicular to the surface. These spectra are representative of the signal-to-noise ratios obtained under normal operating conditions. The spectra have been normalized to a constant value at 330 eV to simplify comparison of intensities. As seen in both spectra, there are no resonances in the carbon continuum at 330 eV. This atomic like fluorescence signal at 330 eV for CO is independent of incident angle or molecular surface orientation and is directly proportional to the total amount of carbon on the surface. The upright, perpendicular configuration of CO was dominant throughout oxidation experiments. This fact was verified by comparing TP-FYNES oxidation experiments (data not shown) done at the carbon continuum, 330.0 eV, and at the π^* resonance, 287.8 eV. Because of this finding, the 287.8 eV resonance was used for all TP-FYNES experiments due to the increased signal-to-noise ratio at this energy.

Temperature-Programmed Fluorescence Yield Near-Edge Spectroscopy. The concentration of available Pt surface sites

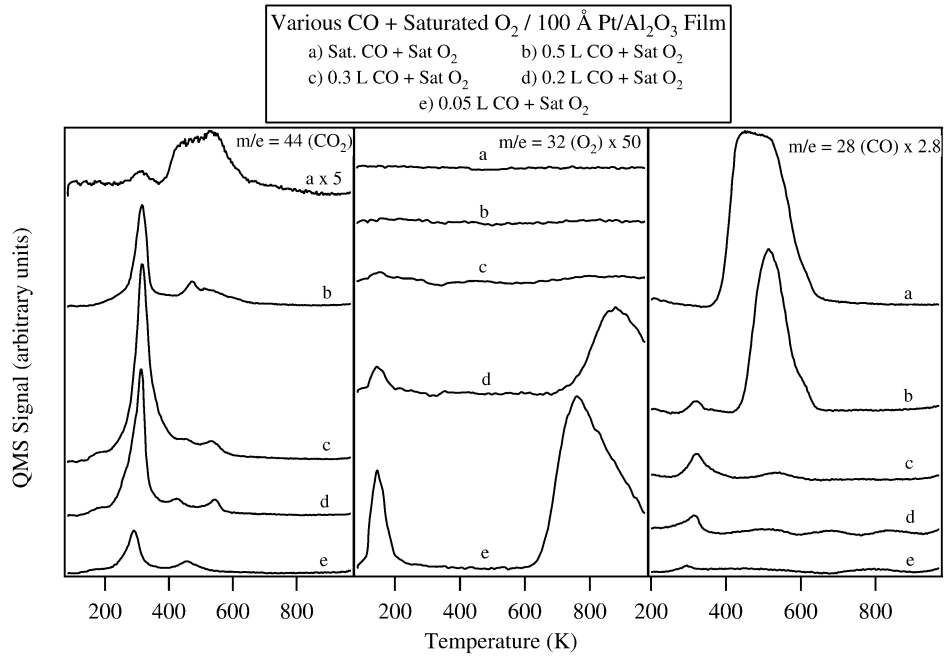

Figure 6. Series of TPRS experiments of selected amounts of preadsorbed CO with a saturation postexposure of oxygen, which illustrates the transition from rich to lean stoichiometry.

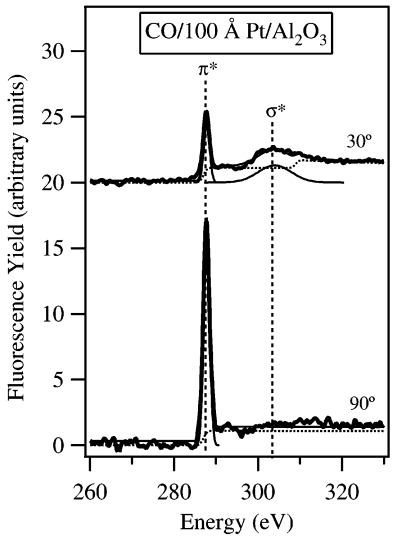

Figure 7. FYNES of CO adsorbed on the 100 Å Pt/350 Å Al_2O_3 thin film acquired at normal (90° to surface plane) and glancing (30° to surface plane) angles. The angular dependence of intensities clearly indicates CO bonds perpendicularly to the film surface.

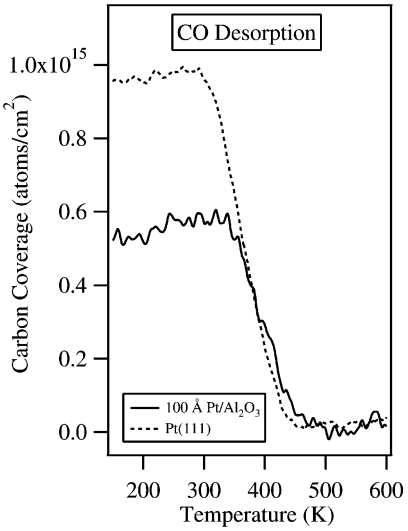

Figure 8. TP-FYNES recorded at 287.8 eV of saturated CO coverages desorbing from Pt(111) and the 100 Å Pt/350 Å Al_2O_3 thin film. Intensities reflect absolute coverages of CO on the surface. The saturation level on the thin film is ~60% of that for the Pt(111) surface.

on this 100 Å Pt/Al_2O_3 thin film has been determined by comparing the fluorescence intensity between a saturated coverage of carbon monoxide on the Pt(111) surface and a saturated coverage of carbon monoxide on the 100 Å Pt/Al_2O_3 thin film. TP-FYNES of saturated CO coverages desorbing from the 100 Å Pt/Al_2O_3 film (solid line) and from the Pt(111) surface (dotted line) is presented in Figure 8. As observed in the trace corresponding to CO desorption from the Pt(111) surface, desorption begins at 305 K and is complete by 450 K. In contrast, CO desorption from the platinum film starts around 345 K and is complete by 450 K. As the coverage decreases with increasing temperature, the higher temperature portion of the CO desorption trace mirrors the trace for CO desorption from Pt(111). Because the absolute carbon concentration for a saturated CO coverage on Pt(111) is known (9.6×10^{14} atoms/cm^2),[38] we estimate the saturation carbon concentration for the platinum film to be 5.8×10^{14} atoms/cm^2, or roughly 60% of the saturation level for the Pt(111) surface by comparing fluorescence levels for the two surfaces.

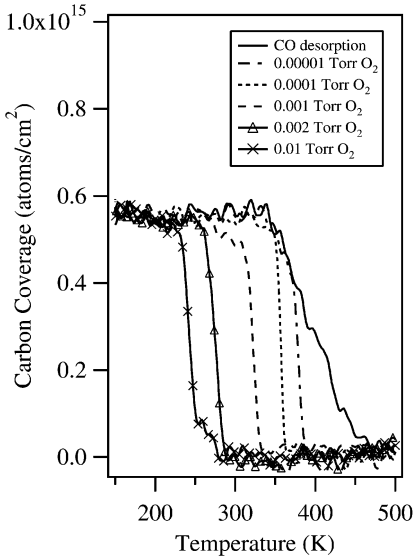

Figure 9. TP-FYNES recorded at 287.8 eV of saturated CO coverages on a 100 Å Pt/350 Å Al_2O_3 thin film heated in selected pressures of flowing oxygen. The onset temperature for oxidation decreases markedly with increasing oxygen pressure.

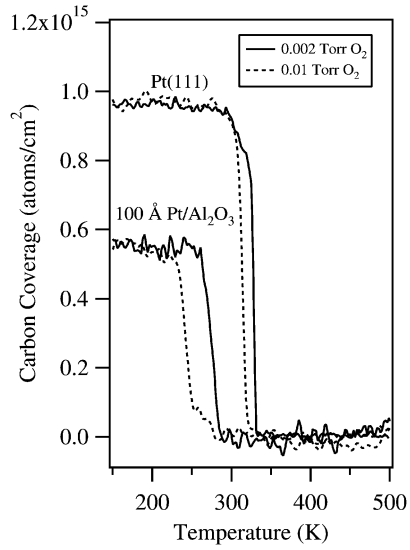

Figure 10. TP-FYNES recorded at 287.8 eV of saturated CO coverages on the Pt(111) surface and the 100 Å Pt/350 Å Al_2O_3 thin film heated in two flowing oxygen pressures. The increase in oxygen pressure has little affect on the onset temperature of oxidation on the Pt(111) surface, whereas for the platinum film the onset temperature of oxidation decreases markedly.

TP-FYNES of CO oxidation experiments on the Pt/Al_2O_3 film has been performed for saturated coverages of CO heated in a wide range of flowing oxygen pressures and are shown in Figure 9. CO desorption (solid trace) is shown for comparison with CO oxidation. As seen in Figure 9, the onset temperature for oxidation decreases markedly with increasing oxygen pressure. When CO is oxidized in 0.00001 Torr of O_2, the onset oxidation temperature is 345 K, whereas the onset oxidation temperature decreases to 230 K when CO is oxidized in 0.01 Torr of O_2. For all oxidation experiments, the CO coverage drops sharply once oxidation begins, and the carbon coverage versus temperature slope remains nearly constant for all oxygen pressures studied.

A comparison of saturated CO coverage oxidation experiments on the Pt(111) surface and on the 100 Å Pt film in 0.01 and 0.002 Torr of oxygen is presented in Figure 10. For Pt(111),

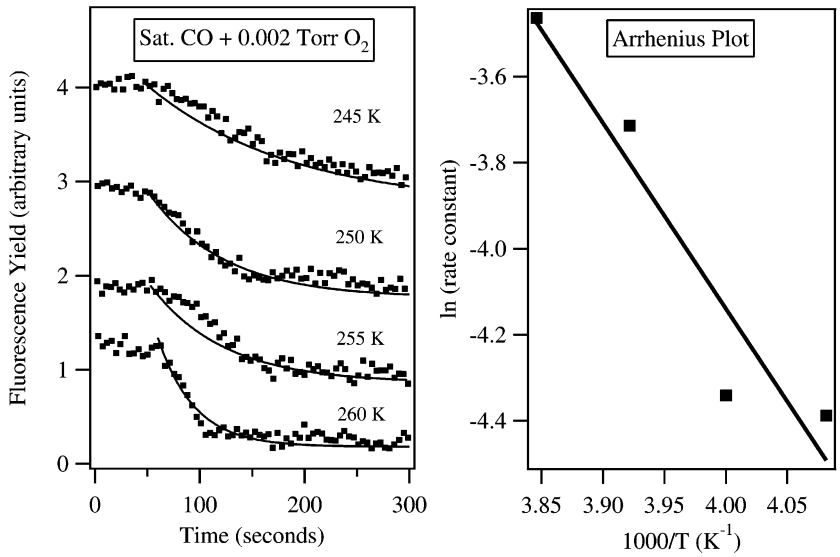

Figure 11. Isothermal FYNES oxidation experiments recorded at 287.8 eV for selected temperatures and in 0.002 Torr of flowing oxygen. All experiments began with a saturated CO coverage at $t = 0$ s and ended with a clean surface by $t = 300$ s. The curves suggest a first-order decay process. Arrhenius plot (right panel), derived from the rate constants extracted from the isothermal experiments shown in the left panel, indicating an activation energy of 8.6 kcal/mol.

the onset temperature for oxidation is virtually unaffected by increasing the oxygen pressure, whereas for the Pt thin film the onset temperature decreases nearly 30 K (from 260 to 230 K) with increasing oxygen pressure. On Pt(111), the onset temperature for oxidation remains at 305 K, which is identical to the temperature for desorption of a saturated CO coverage, as observed in Figure 8. For the platinum film, oxidation is complete by 290 K for both oxygen pressures, whereas for the Pt(111) surface oxidation is not complete until 335 K.

Isothermal FYNES experiments have been performed to determine kinetic parameters for CO oxidation on the 100 Å platinum film. A series of isothermal oxidation experiments over a range of reaction temperatures (from 245 to 260 K) is displayed in the left panel of Figure 11. All experiments began with a saturated CO coverage at $t = 0$ s and ended with a clean surface by $t = 300$ s. The isothermal data have been fit to first-order decay curves from which rate constants were extracted. The rate constant data has been graphed in Arrhenius format (Figure 11, right panel), and the analysis has yielded an 8.6 kcal/mol activation energy with a preexponential factor of 5.1×10^5 s^{-1}.

Discussion

Film Characterization. Through both chemical and structural characterization techniques, a clear picture of the Pt/Al_2O_3 film emerges. TPD, FYNES, and TEM experiments all indicate the film is composed of large, flat platinum grains with a highly textured out of plane orientation corresponding to the Pt(111) direction. Thermal desorption of CO from the 100 Å Pt film (Figure 1) is similar to CO desorption from Pt(111). As seen in Figure 1, CO desorbs from the thin film in a main peak from 350 to 550 K, with the peak maximum at 440 K for a saturated CO coverage (2.0 L exposure). A secondary, high-temperature peak is found from 550 to 620 K, with a peak maximum around 575 K. Previous CO TPD studies on Pt(111) indicate the main CO desorption peak occurs over the 325−500 K temperature range, with the defect peak between 500 and 560 K.[45−49] The maximum peak temperatures for a saturated coverage of CO on Pt(111) range between 420 and 450 K, using heating rates ranging from 10 to 15 K/s.[47−49] In this work, peak temperatures for CO desorption from the Pt thin film are slightly higher than the CO/Pt(111) peak temperatures. Nonetheless, comparing the results in Figure 1 to other studies on platinum single crystals further supports the Pt(111) character of the 100 Å thin film. The CO desorption peak temperatures and shapes in the current research more closely match Pt(111) desorption data in previous research, compared to other crystals faces, Pt(110), Pt(100), Pt(210), and Pt(211), studied.[46] Studies of CO desorption from platinum particles supported on alumina indicate the platinum surface is similar to Pt(111) when the particle size is above ~7.0 nm.[17−19] In this study, the platinum grain size appears to be quite large and the surface is similar to Pt(111), in agreement with the earlier study. Also, CO desorption from the platinum thin film is not dominated by defect sites, as suggested by comparisons to CO desorption data from the following high defect density Pt surfaces: the kinked Pt(321) surface,[50] the stepped Pt(112) surface,[51,52] and the stepped Pt(335) surface.[51,53,54] Yet, comparisons between CO desorption spectra on the Pt(111) surface and the Pt thin film indicate the concentration of defect sites is greater on the thin film. For the Pt thin film, comparison of peak areas for the main CO desorption peak and the high-temperature shoulder indicate an approximate 5% defect site concentration. In summary, CO desorption from the 100 Å platinum film indicates the surface has primarily Pt(111) character.

Oxygen desorption data further support our contention that the platinum thin film has high Pt(111) character. Figure 2 shows a sharp molecular oxygen desorption peak at 141 K and a broad recombinative atomic oxygen desorption peak from 580 to 960 K, both of which are characteristic of oxygen desorption from Pt(111).[41] The recombinative atomic oxygen desorption peak maximum shifts to lower temperatures with increasing coverages, whereas the temperature of the molecular oxygen peak remains unaffected by coverage, also consistent with O_2 desorption from Pt(111). Recently, other researchers in our group performed oxygen desorption experiments on a similar 100 Å platinum film and found that the O_2 desorption from the Pt film resembled desorption from the Pt(111) surface.[36] Oxygen desorption from small platinum particles supported on alumina has also been studied.[10] On these surfaces, the authors determined that the surface behaves like that of the low-index planes with large platinum particle sizes. For 8.3 nm platinum particles

atomic oxygen desorbed in a broad peak between 690 and 950 K, consistent with O(a) desorption experiments from Pt(111).[10] As with CO TPD, oxygen TPD on the 100 Å platinum thin film suggests the surface is nearly Pt(111) in nature.

The CO FYNES shown in Figure 7 indicates that carbon monoxide bonds in an upright configuration, perpendicular to the Pt/Al_2O_3 thin film surface. At normal incidence (90° to surface plane), there is a large π^* resonance at 287.8 eV, whereas the intensity of the σ^* at 303.0 eV is negligible. In the glancing incidence spectrum (30° to surface plane), the π^* intensity decreases whereas the σ^* intensity increases dramatically compared to the intensity in the normal incidence spectrum. An undetectable intensity of the σ^* peak at normal incidence is indicative of CO bonding in an upright configuration.[55,56] The perpendicular geometry of CO adsorbed on the platinum thin film agrees with earlier UPS work performed on alumina-supported platinum, where CO is found to adsorb perpendicularly with the carbon end down, independent of platinum particle size.[18] Because there is no spectroscopic evidence indicating that CO is adsorbed at an angle to the thin film surface, results suggest that the exposed platinum thin film surface is made of Pt terraces parallel to the film substrate.

Structural characterization via TEM clearly reveals the morphology of the platinum film. Cross-section TEM micrographs (Figure 3) indicate the surface of the film is a 100 Å continuous layer of platinum. The platinum layer is parallel to a ~350 Å layer of alumina on top of a thick layer of SiO_2. The lattice fringes in the Pt layer shown by the cross-section TEM micrograph (Figure 3b) indicate the platinum is crystalline. The structure of the Pt film is further resolved by the plane-view TEM images (Figure 4). The bright-field, plane-view image (Figure 4a) reveals a continuous Pt film with an approximate 450 Å average grain size. The orientation of the Pt grains is clearly revealed in the SAD images (insets of Figure 4a,b). Ring indexing (Table 1) using Si(100) as a reference standard reveals several possible platinum planes present that all overlap closely with possible alumina rings. Selected area diffraction from a single grain (Figure 4b) clearly shows the grain has 6-fold symmetry and indexes precisely to a Pt(111) zone axis pattern. This identical and unique diffraction pattern was obtained for all Pt grains investigated. The absence of any Pt(111) or Pt(222) spots in the diffraction pattern combined with the presence of the Pt(220) and Pt(422) planes distinctly suggests that the platinum film is dominated by grains of (111) orientation.

CO Oxidation. The experiments described in this work clearly indicate that CO oxidation on the 100 Å Pt/350 Å Al_2O_3 film occurs in a fashion similar to CO oxidation on the Pt(111) surface. The major difference between the two systems is the role that the increased defect concentration of the thin film plays in the oxidation mechanisms, especially at high oxygen pressures. The TPRS results on the platinum film are similar to results on the Pt(111) surface. On both surfaces, a primary oxidation peak is centered at approximately 315 K. This finding agrees with TPRS studies performed by previous groups.[6,57,58] The authors detected a major CO_2 peak around 315 K and attributed it to the reaction between coadsorbed CO and atomic oxygen on the Pt(111) surface. These comparisons would suggest that a majority of the CO is being oxidized on the large platinum domains with Pt(111) character. Nevertheless, for the Pt(111) surface, there are no oxidation peaks at higher temperatures, such as the small 445 and 530 K CO_2 peaks observed on the platinum film (Figures 5 and 6). As mentioned previously, these high-temperature peaks are likely related to oxidation of tightly bound CO adsorbed on low-coordination Pt sites, and this point is supported by previous experiments on stepped platinum surfaces.[59−65] This high-temperature carbon dioxide formation has also been observed on a Pt/Al_2O_3 monolith catalyst,[12] where in oxygen flow experiments on a CO presaturated catalyst surface a CO_2 formation peak was detected around 450 K. Together, this previous research supports the conclusion that the high-temperature CO_2 peaks are most likely attributed to the oxidation of CO adsorbed at low-coordination platinum sites, or defect sites.

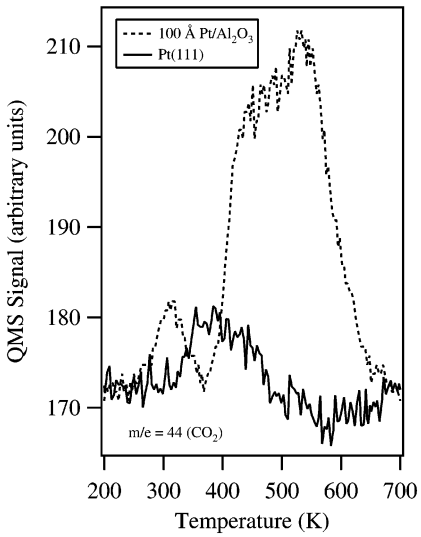

Figure 12. TPRS experiments on two different Pt surfaces of preadsorbed saturated CO coverages coadsorbed with postexposures of oxygen. The increased defect site concentration on the Pt thin film (dashed line) results in more oxygen adsorption and CO_2 formation from the Pt thin film compared to the Pt(111) surface (solid line).

The most significant differences between CO oxidation on the platinum thin film and Pt(111) are illustrated in the TP-FYNES experiments presented in Figures 9 and 10. As mentioned previously, Figure 9 displays the strong dependence of the onset temperature of oxidation for a saturated CO coverage on ambient oxygen pressure. When heated in 0.00001 Torr of oxygen, CO begins oxidation near the desorption temperature for a saturated CO coverage. Yet, when the saturated CO coverage is heated in 0.01 Torr of oxygen, the onset temperature of oxidation decreases dramatically to 230 K. This phenomenon does not occur during oxidation of a saturated CO coverage on Pt(111), as illustrated by Figure 10. For Pt(111), the ambient oxygen pressure has no affect on the onset temperature of oxidation. For all oxygen pressures studied (1×10^{-6} to 1×10^{-2} Torr), the onset temperature of oxidation remains at the saturated CO coverage desorption temperature for Pt(111), indicating that the oxidation reaction is limited by CO desorption.[27,33] Below the ignition temperature the main surface species is atop CO and the reaction rate is inversely proportional to the surface coverage of this species, indicating that atop CO is an inhibitor in the reaction.[27] Previous TP-FYNES studies on partial CO coverages adsorbed on Pt(111) show that increasing oxygen pressures substantially decrease the onset temperature for oxidation, indicating that CO desorption is no longer rate limiting for these reaction conditions.[33]

Still, for high CO coverages, the reaction is not CO desorption limited for the 100 Å platinum film. Small amounts of oxygen adsorb even during low-pressure TPRS experiments with a saturated CO coverage preadsorbed on the surface. This point is highlighted in Figure 12, where carbon dioxide traces from the Pt thin film (dotted line) and the Pt(111) surface (solid line) are compared. In these experiments, a saturated coverage of CO

is preadsorbed on the surface, followed by a postexposure of oxygen. As seen in Figure 12, a larger amount of CO_2 is desorbed from the Pt film compared to the amount desorbed from the Pt(111) surface. These results suggest that the higher defect density on the platinum thin film increases oxygen adsorption, even for a CO saturated surface. The effect of defect sites is magnified in TP-FYNES experiments at higher oxygen pressures. During these TP-FYNES experiments, increasing the oxygen pressure increases the rate of oxidation, indicating increased amounts of oxygen are available for reaction. The adsorption sites, which dominate during low-temperature oxidation, may be located at the edges of platinum grains or may be caused by support-modified platinum sites. TP-FYNES results on the Pt(411) surface (alternating two- and three-atom-wide 100 terraces with 111 steps) also indicate defect sites allow for oxygen adsorption on a CO saturated surface.[66] Taken together, these results indicate defect sites play a key role in CO oxidation on platinum surfaces.

The rate-limiting step for CO oxidation on the Pt thin film is discussed further in the following section based on activation energies determined using isothermal kinetic measurements. The 8.6 kcal/mol activation energy obtained (see Figure 11) for the oxidation of a saturated CO coverage on the 100 Å platinum film is within the range (7.2−15.0 kcal/mol) of previously published CO oxidation experiments below 500 K on Pt/Al_2O_3 catalysts.[16] Similar isothermal experiments were performed on Pt(111) in 0.002 Torr of oxygen, yielding an activation energy of 11.9 kcal/mol for high CO coverages.[33] This CO oxidation activation energy on Pt(111) is similar to the CO desorption energy at high coverages, indicating that the reaction is CO desorption limited on the (111) surface. Conversely, for the 100 Å platinum film the 8.6 kcal/mol activation energy is quite a bit lower than the CO desorption energy on alumina-supported platinum obtained in this research (32.6 kcal/mol) and by previous researchers (29.9 kcal/mol).[19] The large difference between the oxidation activation energy and the CO desorption energy indicates that the oxidation reaction is not CO desorption limited. The prefactor obtained from the Arrhenius plot in Figure 11 is 5.1×10^5 s^{-1}. Performing a Redhead analysis[40] on the 315 K CO_2 peak obtained during TPRS experiments using the prefactor obtained from the isothermal experiments yields an activation energy of 12.9 kcal/mol. Although the Redhead equation is only an approximation, the 12.9 kcal/mol TPRS activation energy compares favorably to the isothermal FYNES experimental value of 8.6 kcal/mol.

Conclusions

CO oxidation has been characterized on a 100 Å Pt/350 Å Al_2O_3 thin film in flowing oxygen pressures up to 0.01 Torr to improve molecular understanding of surface reactions on more complex surfaces under more realistic operating conditions. Using both chemical and structural characterization techniques, the film has been determined to be primarily composed of flat, ∼450 Å Pt grains with (111) orientation and a moderate defect site concentration. These defect sites play a vital role in the oxidation mechanism. Oxidation experiments of saturated CO coverages indicate that the reaction is not CO desorption limited, as it is on the Pt(111) surface. The influence of defect sites is magnified at elevated oxygen pressures. The defect sites increase the amount of oxygen available for reaction, thus substantially lowering the onset temperature for oxidation with increasing oxygen pressures. Even a 5% defect concentration is able to greatly influence CO oxidation mechanisms over a wide pressure range. The results reported here demonstrate the versatility of these in situ soft X-ray techniques in combination with other surface science methods for molecular-level characterization of reaction mechanisms on a variety of catalyst surfaces over a wide range of experimental conditions.

Acknowledgment. We thank the Department of Energy for financial support through Grant DE-FG02-91ER1490. We also thank the University of Michigan Electron Microbeam Analysis Laboratory, especially Dr. Corinna Wauchope, for help with acquiring TEM images. D.J.B. thanks the Rackham Graduate School at The University of Michigan for funding in the form of a Rackham Predoctoral Fellowship. A.L.M. acknowledges the National Science Foundation for support through an IGERT fellowship (Grant DGE−9972776). Part of this research was carried out at the National Synchrotron Light Source, Brookhaven National Laboratory, which is supported by the U.S. Department of Energy, Division of Materials Sciences and Division of Chemical Sciences, under Contract No. DE-AC02-98CH10886. Certain commercial names are identified in this paper for the purpose of clarity in the presentation. Such identification does not imply endorsement by the National Institute of Standards and Technology.

References and Notes

(1) Ertl, G. *Surf. Sci.* **1994**, *299*−*300*, 742.
(2) Rodriguez, J. A.; Goodman, D. W. *Surf. Sci. Rep.* **1991**, *14*, 1.
(3) Zaera, F.; Liu, L.; Xu, M. *J. Chem. Phys.* **1997**, *106*, 4204.
(4) Che, M.; Bennet, C. O. *Adv. Catal.* **1989**, *36*, 55.
(5) Engel, T.; Ertl, G. *Adv. Catal.* **1979**, *28*, 1.
(6) Gland, J. L.; Kollin, E. B. *J. Chem. Phys.* **1983**, *103*, 963.
(7) Harold, M. P.; Garske, M. E. *J. Catal.* **1991**, *127*, 524.
(8) Ree, J.; Kim, Y. H.; Shin, H. K. *J. Chem. Phys.* **1996**, *104*, 742.
(9) Liu, J.; Xu, M.; Zaera, F. *Catal. Lett.* **1996**, *37*, 9.
(10) Putna, E. S.; Vohs, J. M.; Gorte, R. J. *Surf. Sci.* **1997**, *391*, L1178.
(11) Zafiris, G. S.; Gorte, R. J. *J. Catal.* **1993**, *140*, 418.
(12) Thormählen, P.; Skoglundh, M.; Fridell, E.; Andersson, B. *J. Catal.* **1999**, *188*, 300.
(13) Matsushima, T. *Bull. Chem. Soc. Jpn.* **1978**, *51*, 1956.
(14) Racine, B. N.; Sally, M. J.; Wade, B.; Herz, R. K. *J. Catal.* **1991**, *127*, 307.
(15) Serre, C.; Garin, F.; Belot, G.; Marie, G. *J. Catal.* **1993**, *141*, 9.
(16) Venderbosch, R. H.; Prins, W.; van Swaaij, W. P. M. *Chem. Eng. Sci.* **1998**, *53*, 3355.
(17) Altman, E. I.; Gorte, R. J. *J. Catal.* **1988**, *110*, 191.
(18) Altman, E. I.; Gorte, R. J. *Surf. Sci.* **1989**, *216*, 386.
(19) Altman, E. I.; Gorte, R. J. *Surf. Sci.* **1986**, *172*, 71.
(20) Anderson, J. A. *J. Chem. Soc., Faraday Trans.* **1992**, *88*, 1197.
(21) Martinez-Arias, A.; Coronado, J. M.; Cataluna, R.; Conesa, J. C.; Soria, J. *J. Phys. Chem. B* **1998**, *102*, 4357.
(22) Ertl, G. *J. Mol. Catal. A* **2002**, *182*−*183*, 5.
(23) Cremer, P. S.; Su, X.; Somorjai, G. A.; Shen, Y. R. *J. Mol. Catal. A* **1998**, *131*, 225.
(24) Harold, M. P.; Garske, M. E. *J. Catal.* **1991**, *127*, 553.
(25) Zhandov V. P.; Kasemo, B. *Appl. Surf. Sci.* **1994**, *74*, 147.
(26) Fuchs, S.; Hahn, T.; Lintz, H.-G. *Chem. Eng. Proc.* **1994**, *33*, 363.
(27) Su, X.; Cremer, P. S.; Shen, Y. R.; Somorjai, G. A. *J. Am. Chem. Soc.* **1997**, *119*, 3994.
(28) Tsai, P. K.; Wu, M. G.; Maple, M. B. *J. Catal.* **1991**, *127*, 512.
(29) Gabelnick, A. M.; Capitano, A. T.; Kane, S. M.; Fischer, D. A.; Gland, J. L. *J. Am. Chem. Soc.* **2000**, *122*, 143.
(30) Gabelnick, A. M.; Burnett, D. J.; Gland, J. L.; Fischer, D. A. *J. Phys. Chem. B* **2001**, *105*, 7748.
(31) Marsh, A. L.; Burnett, D. J.; Fischer, D. A.; Gland, J. L. *J. Phys. Chem. B* **2003**, *107*, 12472.
(32) Marsh, A. L.; Burnett, D. J.; Fischer, D. A.; Gland, J. L. *J. Phys. Chem. B* **2004**, *108*, 605.
(33) Burnett, D. J.; Capitano, A. T.; Gabelnick, A. M.; Marsh, A. L.; Fischer, D. A.; Gland, J. L. *Surf. Sci.*, submitted for publication.
(34) Hayek, K. *J. Mol. Catal.* **1989**, *51*, 347.
(35) Madou, M. J.; Morrison, S. R. *Chemical Sensing with Solid State Devices*; Academic Press: San Diego, CA, 1989.
(36) Walton, R. M. Mechanistic studies of platinum-titania and platinum-alumina thin films for microchemical gas sensors. Ph.D. Dissertation, University of Michigan, Ann Arbor, MI, 1997.
(37) Fischer, D. A.; Colbert, J.; Gland, J. L. *Rev. Sci. Instrum.* **1989**, *60*, 1596.

(38) Norton, P. R.; Davies, J. A.; Jackman, T. E. *Surf. Sci.* **1982**, *122*, L593.
(39) Gabelnick A. M.; Gland, J. L. *Surf. Sci.* **1999**, *440*, 340.
(40) Redhead, P. A. *Vacuum* **1962**, *12*, 203-211.
(41) Gland, J. L. *Surf. Sci.* **1980**, *93*, 487.
(42) *Standard X-ray Diffraction Powder Patterns*; National Bureau of Standards Monograph No. 25; U.S. Department of Commerce, U.S. Government Printing Office: Washington, DC, 1976.
(43) *Standard X-ray Diffraction Powder Patterns*; National Bureau of Standards Circular No. 539; U.S. Department of Commerce, U.S. Government Printing Office: Washington, DC, 1953.
(44) Huang, T.; Parrish, W.; Masciocchi, N.; Wang, P. *Adv. X-Ray Anal.* **1990**, *33*, 295.
(45) Ertl, G.; Neumann, M.; Streit, K. M. *Surf. Sci.* **1977**, *64*, 393.
(46) McCabe, R. W.; Schmidt, L. D. *Surf. Sci.* **1977**, *66*, 101.
(47) Norton, P. R.; Goodale, J. W.; Selkirk, E. B. *Surf. Sci.* **1979**, *83*, 189.
(48) Hopster, H.; Ibach, H. *Surf. Sci.* **1978**, *77*, 109.
(49) Craig, Jr., J. H. *Appl. Surf. Sci.* **1986**, *25*, 333.
(50) McClellan, M. R.; Gland, J. L.; McFeeley, F. R. *Surf. Sci.* **1981**, *112*, 63.
(51) Xu, J.; Yates, J. T. *Surf. Sci.* **1995**, *327*, 193.
(52) Siddiqui, H. R.; Guo, X.; Chorkendorff, I.; Yates, J. T. *Surf. Sci.* **1987**, *191*, L813.
(53) Lambert, D. K.; Tobin, R. G. *Surf. Sci.* **1990**, *232*, 149.
(54) Luo, J. S.; Tobin, R. G.; Lambert, D. K.; Fisher, G. B.; DiMaggio, G. L. *Surf. Sci.* **1992**, *274*, 53.
(55) Sette, F.; Stöhr, J.; Kollin, E. B.; Dwyer, D. J.; Gland, J. L.; Robbins, J. L.; Johnson, A. L. *Phys. Rev. Lett.* **1985**, *54*, 935.
(56) Stöhr, J. In *NEXAFS Spectroscopy*; Gomer, R., Ed.; Springer Series in Surface Science 25; Springer: New York, 1992.
(57) Matsushima, T. *Surf. Sci.* **1983**, *127*, 403.
(58) Yoshinobu, J.; Kawai, M. *J. Chem. Phys.* **1995**, *103*, 3220.
(59) Szabó, A.; Henderson, M. A.; Yates, J. T. *J. Chem. Phys.* **1992**, *92*, 6191.
(60) Ohno, Y.; Yamanaka, T.; Akiyama, H.; Seimiya, Y.; Matsushima, T. *Appl. Surf. Sci.* **1997**, *121*−*122*, 567.
(61) Ohno, Y.; Sanchez, J. R.; Lesar, A.; Yamanank, T.; Matsushima, T. *Surf. Sci.* **1997**, *382*, 221.
(62) Skelton, D. C.; Tobin, R. G.; Lambert, D. K.; Dimaggio, C. L.; Fisher, G. B. *J. Phys. Chem. B* **1999**, *103*, 964.
(63) Matsushima, T.; Akiyama, H.; Lesar, A.; Sugimura, H.; Torre, G. E. D.; Yamanaka, Y.; Ohno, Y. *Surf. Sci.* **1997**, *386*, 24.
(64) Matsushima, T.; Ohno, Y.; Rar, A. *Surf. Sci.* **1993**, *293*, 145.
(65) Fair, J. A.; Madix, R. J. *J. Chem. Phys.* **1980**, *73*, 3486.
(66) Lewis, H. D.; Gabelnick, A. M.; Burnett, D. J.; Fischer, D. A.; Gland, J. L. *J. Phys. Chem. B*, submitted for publication.